RAP1 and telomere structure regulate telomere position effects in *Saccharomyces cerevisiae*

Gabriele Kyrion,[1,3] Ke Liu,[1–3] Cheng Liu,[1,2] and Arthur J. Lustig,[1,2]

[1]Molecular Biology Program, Sloan-Kettering Institute, Memorial Sloan-Kettering Cancer Center, and [2]Graduate Program in Molecular Biology, Cornell University Graduate School of Medical Sciences, New York, New York 10021 USA

To investigate the role of the yeast telomere-, silencing-, and UAS-binding protein RAP1 in telomere position effects, we have characterized two sets of mutant cells: (1) a set of *rap1* alleles (termed the *rap1^t* alleles) that produce truncated RAP1 proteins missing the carboxy-terminal 144–165 amino acids; and (2) null mutants of the *RIF1* gene, encoding a protein capable of interaction with the carboxyl terminus of RAP1. The data presented here indicate that loss of the carboxyl terminus of RAP1 abolishes position effects at yeast telomeres and diminishes silencing at the *HML* locus. Elimination of position effects in these cells is associated with increased accessibility to the *Escherichia coli dam* methylase in vivo. Thus, the carboxy-terminal domain of RAP1 is required for telomere position effects. In contrast, *rif1* deletion alleles increase the frequency of repressed cells. Using the *rap1^t* alleles to generate wild-type cells differing only in telomere tract lengths, we also show that telomere position effects are highly sensitive to changes in the size (or structure) of the telomeric tract. Longer poly($G_{1-3}T$) tracts can increase the frequency of transcriptional repression at the telomere, suggesting that telomeric poly($G_{1-3}T$) tracts play an active role in the formation or stability of subtelomeric transcriptional states.

[*Key Words*: RAP1; telomere position effects; *dam* methylase; *HML* silencing; RIF1]

Received January 15, 1993; revised version accepted May 11, 1993.

Telomeres, the unique protein–DNA structures present at the termini of linear eukaryotic chromosomes, confer metastable position effects on the transcription of neighboring genes (Levis et al. 1985; Gottschling et al. 1990). In the yeast *Saccharomyces cerevisiae*, genes positioned adjacent to the ends of chromosomes undergo repetitive cycles of activation and repression, with each state maintained for multiple generations (Gottschling et al. 1990). Interestingly, genes subject to these telomere position effects are only weakly accessible to methylation in vivo by exogenously introduced *Escherichia coli dam* methylase, leading to the suggestion that changes in chromatin structure may be associated with these repressive effects (Gottschling 1992). Although telomere position effects appear to require a physical terminus (Gottschling et al. 1990), the involvement of telomeric poly($G_{1-3}T$) tracts in this process has remained unknown.

Telomere position effects share *trans*-acting requirements with the silencing of the cryptic mating-type information present at *HMLα* and *HMR***a** located 12 and 30 kb from the left and right telomeres of chromosome III, respectively (Aparicio et al. 1991; Laurenson and Rine 1992). The repressed state at *HMLα* and *HMR***a** is dependent on the *SIR1*, *SIR2*, *SIR3*, and *SIR4* gene products. Mutations in any one of these four genes lead to derepression of mating-type information. In addition, mutations in the two genes encoding the subunits of the amino-terminal acetyltransferase (*NAT1* and *ARD1*) and amino-terminal deletions of histone H4 result in partial or complete derepression of *HMLα* and *HMR***a**. With the exception of *sir1*, mutations in all of these gene products relieve the repression of telomere-adjacent genes (Aparicio et al. 1991) and, where tested, lead to a deprotection against *dam* methylation in vivo (Gottschling 1992). The common dependence of telomere position effects and HM silencing on these gene products suggests that these two processes may be mechanistically linked. Although telomeric position is not required for HM silencing, it may nonetheless influence this process, as the *cis*-acting requirements for the silencing of *HMLα* on a circular plasmid and at its normal subtelomeric chromosome position are substantially different (Mahoney and Broach 1989; Mahoney et al. 1991).

The UAS-, silencer-, and telomere-binding protein RAP1 has been implicated in the control of HM silencing. Binding sites for this protein are located in the silencer elements present at both *HMLα* and *HMR***a** (Shore et al. 1987). At *HMR***a**, sites for the binding of three activities ABF1, ORC [the activity thought to bind to the

[3]**These authors contributed equally to this study.**

consensus autonomously replicating sequence (ARS) element], and RAP1 are present (Shore et al. 1987; Bell and Stillman 1992; for review, see Laurenson and Rine 1992). Although deletions of any one of these sites do not have a substantial effect on silencing, elimination of any two sites results in the total derepression of this locus (Brand et al. 1987). Direct evidence for a role of RAP1 in silencing at *HMR***a** has been provided by the identification of carboxy-terminal missense mutations of *rap1* (the $rap1^s$ alleles) that, in strains deleted for the consensus ARS element at *HMR* (*HMRΔA*), cause a loss of *HMR* silencing (Sussel and Shore 1991). Overproduction of the carboxyl terminus of RAP1 similarly results in a loss of silencing of the *HMRΔA* silencer, suggesting that a protein interacting with the carboxyl terminus may be titrated in these strains (Hardy et al. 1992a). One such protein, RIF1, has recently been identified (Hardy et al. 1992b). Null mutations in *RIF1* confer $rap1^s$-like phenotypes. The observations that the $Rap1^s$ proteins are defective in their interaction with wild-type RIF1, and that a specific missense allele of *rif1* can suppress this defect, argue for a direct physical association between the carboxyl terminus of RAP1 and RIF1. At the *HMLα* locus, two functionally redundant silencer elements, E and I, are present (Hofmann et al. 1989; Mahoney and Broach 1989; Mahoney et al. 1991; Laurenson and Rine 1992). The E element contains a RAP1-binding site which, when deleted, results in partial derepression of *HML* in strains lacking the I element (Mahoney et al. 1991). Although these data suggest that RAP1 is involved in *HML* silencing, *rap1* mutations affecting *HML* silencing have not yet been identified (D. Shore, pers. comm.).

High-affinity RAP1-binding sites are also present within the poly($G_{1-3}T$) tract of the yeast telomere (Buchman et al. 1988; Longtine et al. 1989). Recent studies have demonstrated that RAP1 binds to the yeast telomere in vivo, where it plays a role in the maintenance of telomere size and stability (Conrad et al. 1990; Lustig et al. 1990; Klein et al. 1992; Kyrion et al. 1992). The role, if any, of RAP1 in telomere position effects has, however, remained unknown. While the $rap1^s$ alleles have substantial effects on *HMR* silencing, these alleles do not influence telomere position effects (E. Wiley and V. Zakian, pers. comm.).

We have recently identified a set of alleles (termed the $rap1^t$ alleles) containing nonsense codons that result in a truncation of the carboxy-terminal 144–165 amino acids of the 827-amino-acid RAP1 protein (Kyrion et al. 1992). Whereas these truncated $Rap1^t$ proteins are capable of specific DNA binding, they have numerous effects on telomere length and stability in vivo. First, the $rap1^t$ mutants display promiscuous telomere elongation, with poly($G_{1-3}T$) tracts increasing in size from 300 bp present in wild type to >4 kb. Second, $rap1^t$ telomeres are highly unstable and are capable of undergoing rapid deletion of up to 3 kb of tract in a single generation. Third, both chromosome loss and nondisjunction are elevated in $rap1^t$ alleles.

Because the carboxyl terminus has been implicated in the silencing function of RAP1, we sought to test whether the terminally truncated $rap1^t$ alleles influence either telomere position effects or *HMLα* silencing. Our results demonstrate that a carboxy-terminal function of RAP1 is an absolute requirement for telomere position effects. We also demonstrate that the structure of the telomere tract itself can influence the efficiency of telomere position effects.

Results

Deletion of the carboxyl terminus of RAP1 results in loss of telomere position effects

To investigate the role of RAP1 in telomere position effects, we tested the ability of cells containing a mutation in one of the $rap1^t$ alleles, *rap1-17*, to repress the *URA3* gene when introduced adjacent to the telomeric tract on either the right arm of chromosome V (V_R) or the left arm of chromosome VII (VII_L). The *rap1-17* gene encodes a protein that, while able to bind specifically to its cognate site, is missing the terminal 165 amino acids (Kyrion et al. 1992). The frequency of $ura3^-$ cells was assayed by determining the fraction of cells capable of growth on medium containing 5-fluoro-orotic acid (5-FOA), a uracil analog that allows the growth of $ura3^-$, but not $URA3^+$, cells (Fig. 1; Table 1). In this genetic background, wild-type *RAP1* cells containing *URA3*-marked V_R and VII_L telomeres give rise to FOA-resistant colonies at median frequencies of 1% and 52%, respectively [Table 1; *RAP1* (Chr)]. A similar context-dependent difference in the FOA^r frequencies of these telomeres has been described previously (Gottschling et al. 1990). In contrast, *rap1-17* cells produce colonies on FOA medium only rarely ($<1 \times 10^{-7}$) at both V_R and VII_L ends [Table 1; *rap1-17* (Chr)]. This phenotype is not the consequence of a general defect in the ability of these strains to grow on FOA-containing medium, because 100% of *rap1-17 ura3-1* cells are FOA^r (Fig.1; data not shown). Cells containing the *rap1-18* allele, which encodes a protein missing the terminal 144 amino acids, also display a marked reduction in the frequency of FOA^r colonies, arising at a frequency of 8×10^{-6}. The magnitude of *URA3* derepression observed in *rap1-17* and *rap1-18* cells is similar to that observed for mutations in the *SIR2* gene (Fig. 1; Table 1; Aparicio et al. 1991). We have observed no differences from wild-type expression when *URA3* is placed at internal positions in these strains (Fig. 1). Derepression of telomeric genes is recessive. Diploids heterozygous for *rap1-17* display wild-type frequencies of FOA^r colonies (Table 1, bottom).

Three lines of evidence indicate that the observed derepression of *URA3* is the consequence of the *rap1-17* mutation. First, loss of telomere position effects is tightly linked genetically to *RAP1*: Following crosses between $rap1^t$ and wild-type cells, only $rap1^t$ spore colonies containing the marked telomere are fully sensitive to FOA (data not shown). Second, replacement of a wild-type copy of *RAP1* with the *rap1-17* gene by a plasmid shuffle (Kyrion et al. 1992) is sufficient to confer *URA3* derepression (Table 1). While strains carrying the wild-

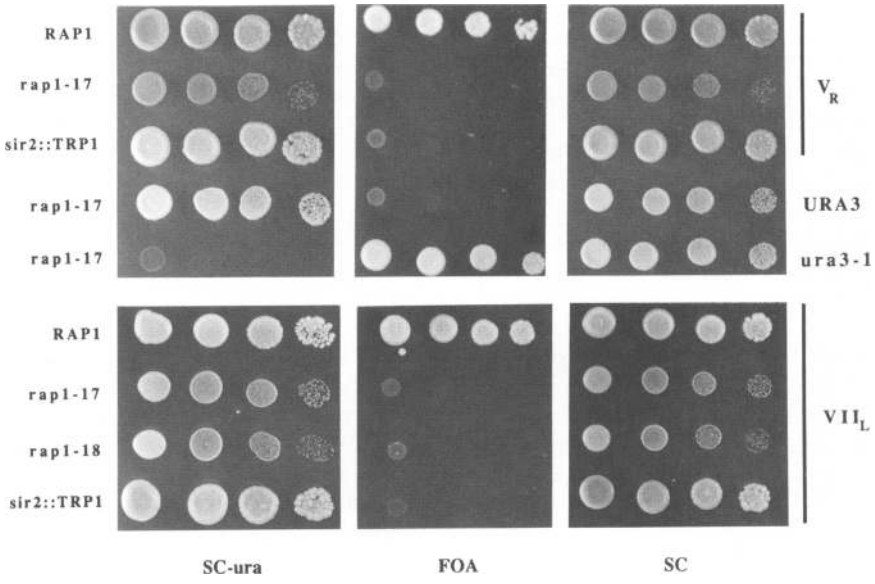

Figure 1. *rap1-17* and *rap1-18* mutations derepress *URA3* expression at the telomere. Serial 10-fold dilutions of wild-type, *rap1-17*, *rap1-18*, and *sir2::TRP1* strains containing *URA3*-marked V_R or VII_L telomeres were plated onto uracil omission media (SC−ura), FOA-containing media (FOA), and synthetic complete media (SC) and grown at 30°C. Also plated are an unmarked *ura3-1 rap1-17* strain and a *rap1-17* strain carrying *URA3* at an internal position on chromosome VII. The *rap1-17* and *rap1-18* strains, although slower growing, have wild-type levels of viability on SC media. Strains used are as follows (*top* to *bottom*): KL4-5b, KL5-2c, KL4-5bΔsir2, AJL364-1c, AJL278-4d, AJL275-2a–VII_L–URA, AJL369-5b, AJL399-4b, and AJL387-5aΔsir2.

type copy of *RAP1* on a centromeric plasmid form colonies on FOA medium at a median frequency of 4×10^{-4}, replacement of the wild-type copy with the *rap1-17* gene generates cells that are fully sensitive to FOA [Table 1, cf. *RAP1* (plasmid) and *rap1-17* (plasmid)]. Third, the presence of a wild-type *RAP1* gene on a CEN plasmid fully complements the effects of an integrated copy of *rap1-17* on gene expression at VII_L (Table 1, *rap1-17/RAP1*).

To confirm that the FOA assay measures differences in *URA3* expression, we compared the levels of *URA3* transcripts produced in wild-type and *rap1-17* strains carrying both a *URA3*-marked telomere at VII_L and a deletion allele of *URA3*, *ura3Δ1*, at its normal locus on chromosome V (Fig. 2). The level of *URA3* mRNA in logarithmically growing cells was determined by Northern analysis. Cells wild-type for *RAP1* contained telomeric *URA3* mRNA at levels below detection (Fig. 2, lane 1). A similarly high level of telomeric repression has been described previously (Aparicio et al. 1991) and is the likely consequence of a reduction in the abundance of transcripts in the fraction of cells that express *URA3*. In contrast, *rap1-17* cells produced these transcripts at levels close to those found in strains carrying only the *ura3-1* allele (Fig. 2, lanes 2,3). We estimate a difference of >10-fold between the level of telomeric transcripts in wild-type and *rap1-17* cells, similar to the derepression observed in other mutants defective in telomere position effects (Aparicio et al. 1991). In contrast, mRNA levels from the *ura3-1* locus were identical in both wild-type and *rap1-17* strains (Fig. 2, lanes 4,5).

To test whether the effect of *rap1^t* alleles on telomere position effects is specific to the *URA3*-marked telomeres, we introduced the *ADE2* gene adjacent to the telomeric tract on chromosome VII_L (Fig. 3, top). The repressed and derepressed states were subsequently monitored visually through the production of red and white sectors, respectively (Gottschling et al. 1990). In this genetic background, ~10% of cells wild-type for *RAP1* and containing a telomeric *ADE2* gene produced white colonies with red sectors. A smaller fraction (~2%) formed red colonies with white sectors (Fig. 3, upper left; Fig. 6, below). In contrast, of >5000 *rap1-17* colonies assayed, all but 1 produced a white colony color, and none of these were capable of forming red sectors (Fig. 3, upper right), indicating that these cells cannot repress *ADE2* expression at the telomere.

Derepression of telomeric gene expression in rap1-17 *cells is independent of poly(G_{1-3}T) tract length*

Recent studies have indicated that the strength of position effects at the telomere is inversely proportional to the distance of the gene from the telomere, with the frequency of repressed states decreasing with increasing distance (Renauld et al., this issue). This effect may be the consequence of an increased distance either between the gene and the beginning of the telomere tract or between the gene and the physical end of the chromosome. One possible explanation of our data, therefore, is that the extended telomere tract in *rap1^t* cells eliminates telomere position effects by increasing the distance between the marker gene and the chromosomal terminus.

To test this hypothesis, we examined *URA3* expression in wild-type spore colonies inheriting elongated *rap1-17* telomeres from heterozygous diploids (see Materials and methods). Wild-type strains inheriting V_R telomeres of ~1.4 kb nonetheless produced a high frequency of FOA^r colonies, indicating that increased telomere length alone is insufficient to explain the loss of position effects [Table 1, cf. *RAP1* (Chr)–300 bp with *RAP1* (Chr)–1370 bp]. A similar result was obtained when a series of plasmid shuffles was used to generate a set of isogenic wild-type and *rap1-17* strains differing

Table 1. *FOA^r frequencies in* rap1^t *cells carrying* URA3*-marked telomeres*

URA3 locus	Genotype[a] (site)	Tract size[b] (bp)	Fraction FOA^r (range of values; number of colonies)[c]
V_R	*RAP1* (Chr)[d]	300	1.1×10^{-2} (0.03–6.5; 30)
	RAP1 (Chr)[d,e]	1370	3.2×10^{-2} (0.006–25; 24)
	RAP1 (plasmid)[f]	350	4.3×10^{-4} (0–63.0; 16)[g]
	RAP1 (plasmid)[f]	1100	5.8×10^{-4} (3.3–35; 8)
	rap1-17 (Chr)	700–2000	$<1.0 \times 10^{-7}$ (16)
	rap1-17 (plasmid)	650	$<1.6 \times 10^{-7}$ (8)
	sir2::TRP1 (Chr)	300	$<1.0 \times 10^{-7}$ (20)
VII_L haploids	*RAP1* (Chr)		5.2×10^{-1} (3.4–7.8; 15)
	rap1-17 (Chr)		$<1.0 \times 10^{-7}$ (26)
	rap1-17 /RAP1 (Chr/plasmid)		4.0×10^{-1} (2.5–7.6; 10)
	rap1-18 (Chr)		8.4×10^{-6} (0–151; 15)[h]
	sir2::TRP1 (Chr)		$<1.5 \times 10^{-7}$ (10)
VII_L diploids	*RAP1/RAP1*		3.7×10^{-1} (3.5–5.6; 5)
	RAP1/rap1-17		2.5×10^{-1} (2.3–4.8; 5)
	rap1-17/rap1-17		$<1.7 \times 10^{-7}$ (10)

[a](Chr) Chromosomal *rap1* allele; (plasmid) *rap1* allele on a CEN plasmid in a strain containing a *rap1::LEU2* disruption at its chromosomal locus.
[b]Average poly($G_{1-3}T$) tract length is presented. In the case of *rap1-17* strains, the average length varied in different strains and subculturings between 700 and 2000 bp.
[c]Observed FOA^r frequencies are presented as median values, with the range of values and the number of colonies assayed in parentheses.
[d]RAP1 (Chr)–300 and RAP1 (Chr)–1370 represent isogenic wild-type strains differing only in tract size.
[e]Pooled data from strains 383-3c s0, 384-1c, and 384-4a presented in Table 2.
[f]RAP1 (plasmid)–350 and RAP1 (plasmid)–1100 represent isogenic wild-type strains derived from a plasmid shuffle and differ only in telomere tract size.
[g]Of the 16 colonies tested, 2 failed to yield any FOA^r cells in the population tested (0/8,800 and 0/12,400).
[h]Of the 15 colonies tested, 1 failed to yield any FOA^r cells in the population tested ($0/1.3 \times 10^7$).

only in the length of the *URA3*-marked V_R telomere. Following a plasmid shuffle, wild-type cells inheriting elongated telomeres from *rap1-17* cells displayed FOA^r rates close to the progenitor wild-type strain, despite their increased tract length [cf. Table 1, *RAP1* (plasmid)–350 bp with *RAP1* (plasmid)–1110 bp]. An additional indication that telomere tract size is not responsible for the effects of the *rap1^t* mutations on telomere position effects is the finding that *rap1-17* cells are completely defective in conferring the repressed state regardless of telomeric length (Table 1).

On the basis of these results, we conclude that loss of the carboxyl terminus of RAP1 in *rap1-17* and *rap1-18* alleles results in the derepression of telomerically located genes in a process that appears to be independent of either the identity of the telomere (V_R or VII_L), the gene examined (*URA3* or *ADE2*), or the length of the telomeric tract.

HMLα *is partially derepressed in* rap1-17 *cells*

Given the profound reduction of telomere position effects in *rap1-17* alleles, we sought to determine whether *HML* silencing is also disrupted in these cells. To directly test for the derepression of *HML*α, we isolated RNA from wild-type, *rap1-17*, and *sir2* cells and analyzed the expression of α1, α2, and **a**2 transcripts in these cells by Northern analysis (Fig. 4). As expected, wild-type *MAT*α cells expressed only α1 and α2 transcripts (Fig. 4, lanes 6,7), whereas only *MAT***a** cells expressed **a**2 message (Fig. 4, lanes 1–5). In contrast, α transcripts were detected for all *rap1-17 MAT***a** strains tested (Fig. 4, lanes 2–4) at levels close to those found in *sir2 MAT***a** cells (Fig. 4, lane 10), indicating that *HML*α is transcriptionally derepressed in *rap1-17* cells. The derepression of α tran-

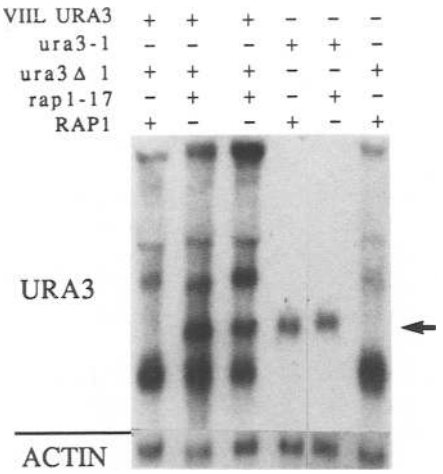

Figure 2. *rap1^t* alleles derepress transcription of *URA3*-marked telomeres. RNA was isolated from *rap1-17* and wild-type strains containing either the *ura3-1* or *ura3Δ1* allele at its normal locus in the presence or absence of the *URA3*-marked VII_L telomere, and subjected to Northern analysis using a probe to the *URA3* gene. The presence (+) or absence (−) of each of the alleles of *URA3* and *RAP1* is indicated at *top*. In addition to the 800-nucleotide *URA3* transcript, indicated by the arrow, multiple species derived from transcription initiating within the *ura3Δ1::TRP1::ura3Δ1* duplication were also observed. To measure the relative levels of RNA in each lane, blots were stripped and rehybridized with a probe to actin RNA, and the hybridization signal was quantitated using the β-scope (Betagen). Control actin mRNA levels in each lane varied by less than twofold. Strains used (in order of lanes) are as follows: AJL401-9c, AJL406-3d, AJL406-4d, AJL401-5a, AJL406-7b, and AJL401-2c.

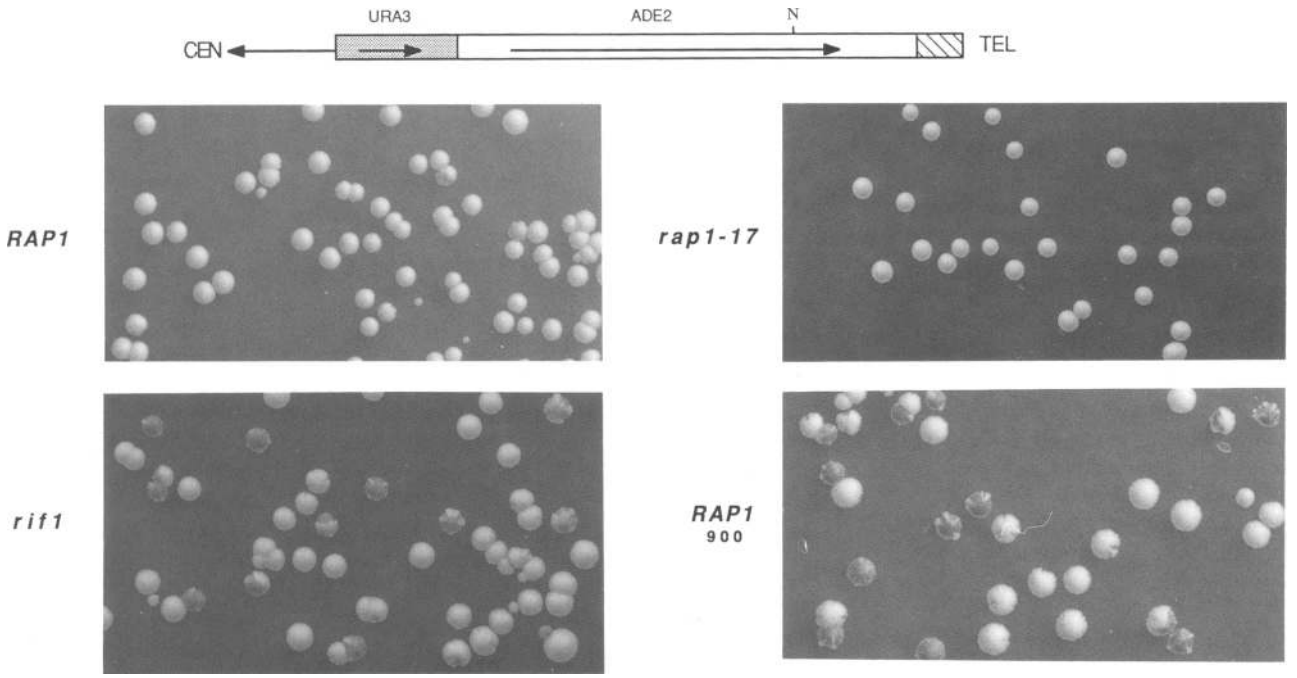

Figure 3. Telomeric *ADE2* expression in wild-type, *rap1-17*, and *rif1* strains. Shown are representative samples of wild-type (*RAP1*, AJL275-2a–VII_L–ADE), *rap1-17* (AJL394-1a), and *rif1::URA3* (AJL396-6a) cells containing an *ADE2*-marked VII_L telomere (shown at *top*) plated on low adenine-containing media after nonselective growth. Also shown is an identical plating of wild-type cells inheriting a 900-bp telomeric tract ($RAP1_{900}$, AJL412-5a), 600 bp longer than the 300-bp tract found in the progenitor wild-type cells. Identical results were obtained with multiple *rap1-17* and *rif1::URA3* strains. The direction of transcription is indicated by the arrows within the *URA3* and *ADE2* genes in the diagram (derived from Gottschling et al. 1990) The position of the *Nde*I site (N) is also indicated.

scripts is fully complemented by a plasmid-borne copy of the *RAP1* gene (Fig. 4, lane 5). This derepression of α1 and α2 transcription is *HML* specific. Transcription of the *MAT*α locus is not affected severely by the *rap1-17* mutation, with transcript levels increasing by no more than twofold from expected values (Fig. 4, lanes 6–9). The *rap1-17* mutation does not significantly derepress *HMR***a**. Both wild-type and *rap1-17* cells do not express detectable levels of **a**2 message.

Consistent with the transcriptional derepression of *HML*α, the mating efficiency of *rap1-17 HML*α *MAT***a** *HMR***a** strains is significantly decreased. Whereas wild-type cells repressed for *HML*α expression display high levels of mating (62%), *rap1-17* cells exhibit 2- to 200-fold lower mating efficiencies, with the extent of the decrease varying widely both among different isogenic *rap1-17* strains and among different colonies derived from a common *rap1-17* progenitor. In contrast, *rap1-17 HML***a** *MAT***a** *HMR***a** strains mate at wild-type efficiencies (data not shown), indicating that derepression of *HML* is required for the lowered mating efficiency. As expected, *rap1-17 HML*α *MAT*α *HMR***a** cells mate at wild-type efficiencies. These data suggest that *HML*α, but not *HMR***a**, is partially derepressed in *rap1-17* cells.

Increased accessibility of E. coli dam *methylase to subtelomeric chromatin in* rap1-17 *cells*

Recent studies have used the accessibility of chromosomal sequences to *dam* methylase as an in vivo assay for chromatin structure (Gottschling 1992; Singh and Klar 1992). Two GATC sites have been identified in the *URA3* gene that display unique characteristics when placed adjacent to telomeric sequences in wild-type strains (Gottschling 1992; Wright et al. 1992). One site, at the junction between *URA3* and poly($G_{1-3}T$) sequences (Fig. 5, site 1), displays hypersensitivity to methylation, whereas a second site within the coding region of *URA3* (Fig. 5, site 2) is only weakly accessible to methylation. The accessibility of site 2 to methylation is regained in strains defective for telomere position effects (e.g., *sir2* mutants), suggesting that the formation of a closed chromatin state may be mechanistically linked to the transcriptionally repressed state at the telomere (Gottschling 1992).

Because *rap1-17* and *sir2* cells display similar levels of *URA3* derepression, we tested whether these strains also exhibit similar changes in accessibility to the *dam* methylase. To this end, a series of isogenic wild-type, *rap1-17*, and *sir2* strains were constructed, each of which contained an integrated copy of the *E. coli dam* methylase gene and a *URA3* gene adjacent to either the V_R or VII_L telomere. To determine the methylation state of site 2, DNA was digested first with *Hin*dIII and *Bam*HI, releasing a 1.15-kb internal fragment containing the *ura3-1* gene (fragment A) and a 1.10-kb telomeric *URA3*-containing fragment (fragment B), and subsequently cleaved with *Mbo*I, *Dpn*I, or *Sau*3AI (Fig. 5). *Mbo*I and *Dpn*I

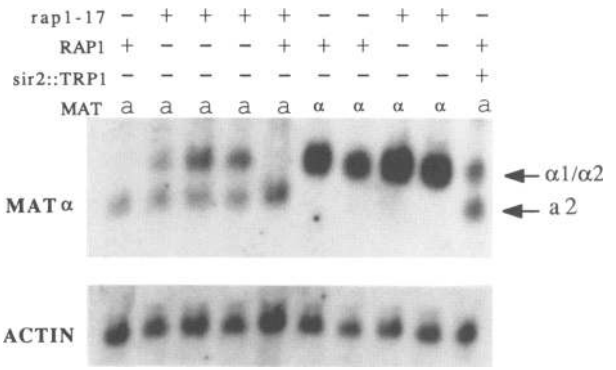

Figure 4. Transcription of *HML*α is derepressed in *rap1-17* cells. RNA was isolated from *MAT***a** and *MAT*α derivatives of wild-type *RAP1*, *rap1-17*, and *sir2::TRP1* cells, and the resulting blots were probed with a restriction fragment containing the *MAT*α gene. This probe hybridizes to both the α1 and α2 transcripts (expressed at the *MAT*α locus) as well as the partially homologous **a**2 transcript (expressed at the *MAT***a** locus). The presence (+) or absence (−) of *rap1* and *sir2* alleles and the mating type of each strain is shown above each lane. (*Top*) The relative abundance of the 740-nucleotide α transcripts (α1/α2) and the 590-nucleotide **a**2 transcript. As a loading control, blots were stripped and hybridized with a probe to actin mRNA (*bottom*). Signals were quantitated using the β-scope (Betagen). α1/α2 Levels were normalized to actin mRNA levels and expressed relative to the *MAT*α wild-type control in lane 6. Relative values are as follows: (Lane 2) 0.23; (lane 3) 0.46; (lane 5) 0.42; (lane 6) 1.0; (lane 7) 1.4; (lane 8) 2.5; (lane 9) 1.8; (lane 10) 0.35. The relative abundance of the **a**2 transcript did not differ between wild-type and *rap1-17 MAT***a** cells, and the **a**2 transcript could not be detected in either wild-type or *rap1-17 MAT*α cells. Taking into account the expected derepression of *HML*α in *rap1-17 MAT*α cells, we estimate that the expression of α1 and α2 at the *MAT*α locus is increased by no more than twofold in *rap1-17* cells. The mating efficiencies of the *MAT***a** strains shown, relative to W303a, are 0.55 (AJL274-4c), 0.12 (AJL278-4d), 0.03 (AJL369-4d), and 1.15 (AJL369-4d/RAP1). Strains used are as follows (in order of lanes): W303a, AJL274-4c, AJL278-4d, AJL369-4d, AJL369-4d/RAP1, W303α, AJL274-3c, AJL278-1a, AJL274-1c, AJL387-5aΔsir2.

cleave at fully unmethylated and fully methylated GATC sites, respectively, whereas *Sau*3AI cleaves GATC regardless of its methylation state. Telomere-specific inaccessibility to methylation is indicated by a preferential retention of fragment B relative to fragment A after digestion with *Dpn*I.

Wild-type cells marked at the VII_L telomere gave results consistent with previous studies (Gottschling 1992; Fig. 5, upper left). Under conditions in which the internal fragment A is efficiently cleaved by *Dpn*I, 70–95% of the telomeric fragment B is resistant to cleavage by *Dpn*I, consistent with a high level of protection against methylation at the telomere. *rap1-17* cells produced a markedly different pattern (Fig. 5, right). Only a subpopulation of fragment B molecules (~15–30%) is resistant to cleavage by *Dpn*I, indicating that the *rap1-17* mutation decreases the susceptibility of site 2 to methylation. However, while less resistant than wild-type, fragment B reproducibly shows less accessibility to the methylase than fragment A. These data suggest that elements of structure responsible for the telomere-specific protection are maintained in *rap1-17* cells. At the V_R telomere, which confers weaker position effects on *URA3* than the VII_L telomere, both wild-type and *rap1-17* cells display levels of telomere–specific protection similar to that found in *rap1-17* cells at the VII_L telomere (data not shown).

It was surprising that telomere-specific protection against methylation was observed in a fraction of *rap1-17* cells despite the phenotypically complete derepression of the telomeric *URA3* gene. To examine whether this property is shared by other mutations affecting telomere position effects, we compared the protection patterns of *rap1-17* and *sir2* mutants containing telomeres marked at VII_L (Fig. 5, lower left). In spite of the identical phenotypes displayed by *rap1-17* and *sir2* cells in the FOA assay, *sir2* cells exhibit a complete loss of telomere-specific protection against methylation. In these mutants, fragment B retains only a residual level of protection also found at the internal locus. An identical result was obtained in *sir2* mutants marked at V_R (data not shown). Hence, whereas both *sir2* and *rap1-17* mutations cause significant changes in subtelomeric chromatin structure, *rap1-17* cells retain a significant degree of protection against the *dam* methylase.

We note that in both wild-type and *rap1-17* cells, the amount of fragment B generated after cleavage with *Hin*dIII and *Dpn*I is only slightly less (~60-95%) than that retained after triple digestion with *Hin*dIII, *Dpn*I, and *Bam*HI. Because *Bam*HI quantitatively cleaves at site 1, these results indicate that the majority of molecules resistant to *Dpn*I at site 2 are cleaved by this enzyme at site 1, suggesting that site 1 is highly accessibile to *dam* methylase in both wild-type and mutant cells.

Loss of RIF1 enhances telomere position effects

One possible cause for the derepression of telomeric genes observed in *rap1*^{t} cells is the absence of specific contacts between the carboxyl terminus of RAP1 and other proteins involved in this process. One candidate for such a factor is RIF1, identified in a genetic screen for carboxyl terminus-interacting proteins (Hardy et al. 1992b). Deletion of the *RIF1* gene results in two phenotypes: derepression of silencing in strains containing *HMRΔA* silencers and elongation of the telomeric tract by 150–300 bp (Hardy et al. 1992b; see Fig. 6). Although phenotypically distinct from *rap1*^{t} alleles with regard to telomere length and stability, the inability of RIF1 to interact with the *Rap1*^{t} protein may nonetheless be partially or completely responsible for their effects on telomere position effects.

To test this possibility, we analyzed the red/white sectoring patterns in a strain carrying a *rif1::URA3* null allele and a subtelomeric *ADE2* gene at chromosome VII_L. Strains carrying the *rif1::URA3* allele sectored at high frequency (Fig. 3, lower left), with 31% of cells forming white colonies with red sectors. Nonetheless,

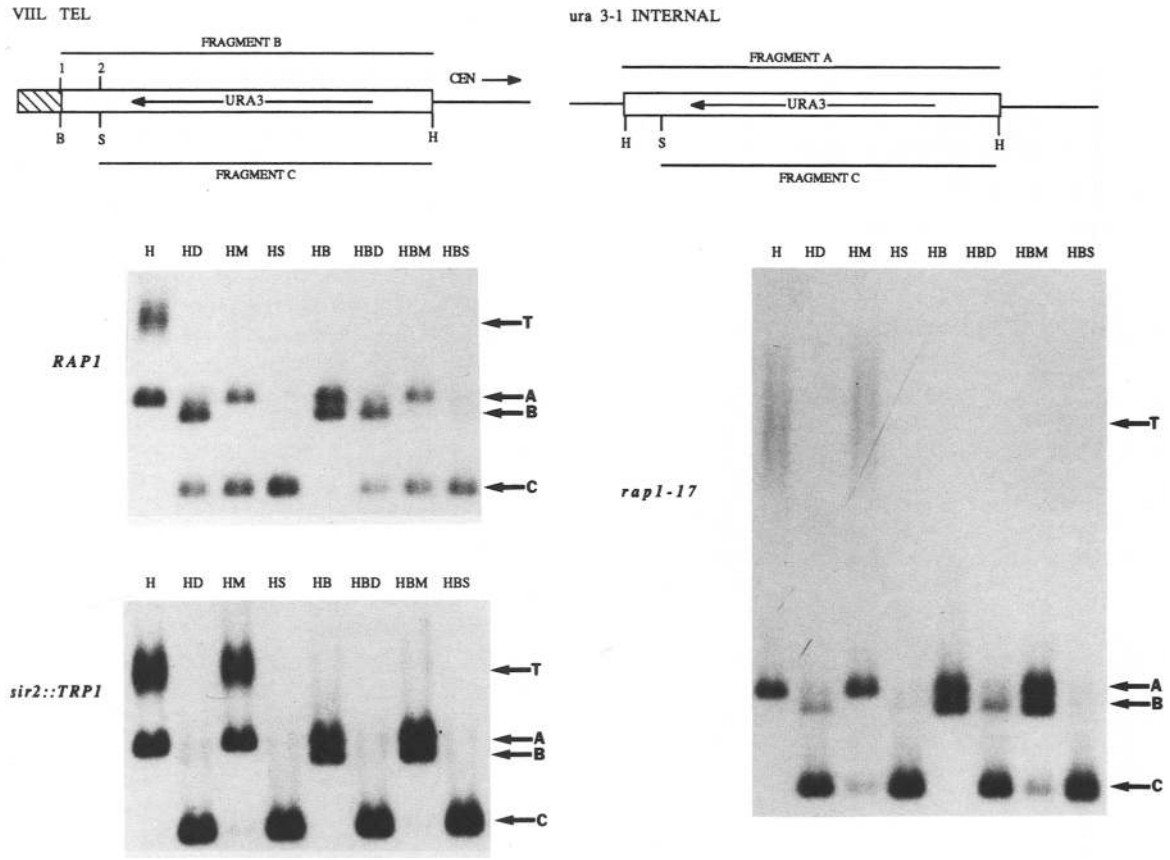

Figure 5. Reduced accessibility of telomeric chromatin to *E. coli dam* methylase in *rap1-17* mutant cells. (*Top*) Diagram of the structure of the *URA3* gene at the VII_L telomere and the *ura3-1* gene at the internal locus (derived from Wright et al. 1992). Diagram designations: (1) The GATC site present at the junction between telomeric sequences (hatched box) and *URA3* sequences; (2) the GATC site present within the coding sequence of the *URA3* gene at VII_L. The GATC sequence at site 1 overlaps a *Bam*HI restriction site. The sources of fragments A, B, and C are shown adjacent to the relevant restriction sites. The direction of *URA3* transcription is shown by the arrow. (*Bottom*) DNAs isolated from wild-type (RAP1, AJL387-5a), *rap1-17* (AJL391-1c), and *sir2::TRP1* (AJL387-5aΔsir2) cells were digested with the restriction enzymes indicated above each lane, and Southern blots were probed with *URA3* sequences. The positions of fragments A, B, and C are indicated by arrows at *right*. The position of the telomeric *Hin*dIII fragment is also indicated by an arrow (T). The *sir2::TRP1* panels were overexposed to demonstrate the absence of any telomere-specific protection in these cells. These results were reproduced in multiple wild-type, *rap1-17*, and *sir2* strains. Abbreviations used are (H) *Hin*dIII; (B) *Bam*HI; (S) *Sau*3A1; (D) *Dpn*I; (M) *Mbo*I; (TEL) telomere; (CEN) centromere.

rif1::URA3 cells displayed a sectoring phenotype distinct from wild-type. Two classes only rarely found in wild-type cells, red colonies with white sectors and unsectored red colonies, were found at elevated frequencies (~10% each). Furthermore, the frequency of white colonies with red sectors was reproducibly two- to three-fold higher than in wild-type cells. In contrast, neither wild-type cells nor *rif1* mutants displayed red/white sectoring patterns when *ADE2* was introduced at a chromosome–internal position at *HIS4* (data not shown). Hence, elimination of RIF1 association with the carboxyl terminus of RAP1 cannot be responsible for the phenotypes observed in *rap1-17* and *rap1-18* cells. The hyper-repressed state in *rif1* cells requires the carboxyl terminus of RAP1, because *rif1::URA3 rap1-17* double mutant cells have a phenotype indistinguishable from *rap1-17* single mutants (1 red sector of 2900 colonies assayed).

Telomere position effects are influenced by the structure of the telomeric tract

The ability to generate *rap1-17* cells with telomeres of varying sizes allowed us to explore the effect of telomere tract size on telomere position effects in wild-type cells (Figs. 3 and 6; Table 2). For these studies, *rap1-17* cells containing marked VII_L or V_R telomeres of differing tract sizes were crossed with wild-type cells. Wild-type spore colonies inheriting telomeres of differing sizes were then examined for their ability to repress the *ADE2* gene at VII_L or the *URA3* gene at V_R. This approach was made possible by the observation that, except for the rapid deletion events noted below, telomeres inherited by wild-type cells decrease in size only slowly (~2 bp per generation, data not shown). Interestingly, increased telomere tract size appears to enhance the frequency of repressed

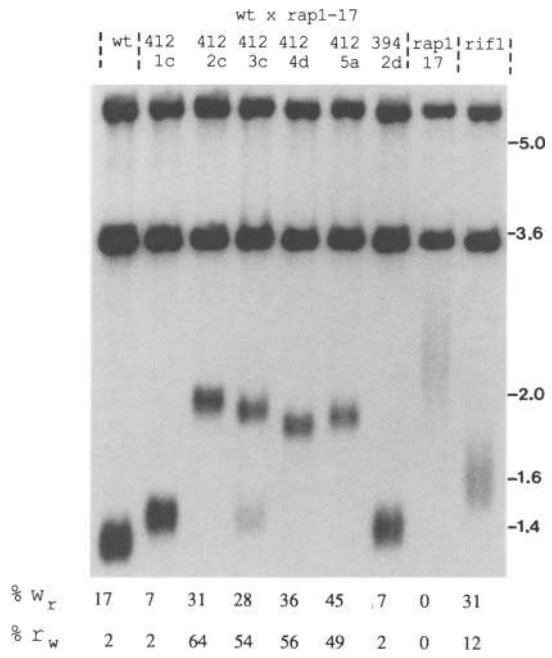

Figure 6. Increased telomere length enhances telomere position effects in wild-type cells. The telomeric fragment sizes of wild-type, *rif1*, and *rap1-17* strains carrying the *ADE2*-marked VII_L telomere are displayed together with quantitation of their sectoring patterns. (wt) The original wild-type strain (AJL275-2a–VII_L–ADE) carrying the *ADE2*-marked VII_L telomere. AJL394-2d is a wild-type spore colony derived from a cross between AJL275-2a–VII_L–ADE and an unmarked *rap1-17*-containing strain. AJL412-1c, -2c, -3c, -4d, and -5a are wild-type spore colonies derived from a cross between an unmarked wild-type strain and a *rap1-17* strain carrying elongated *ADE2*-marked telomeres. *ADE2*-marked *rap1-17* (AJL394-1d) and *rif1::URA3* (AJL395-1d) mutant cells are also shown at *right*. DNAs isolated from these strains were digested with *Nde*I, which distinguishes between the internal and telomeric *ADE2* alleles (see Fig. 3), and the resulting blots hybridized to an *ADE2* probe. The two high-molecular-mass species reflect subtelomeric and internal fragments of *ADE2*. The percentages of each population displaying white colonies with red sectors (%w_r) and red colonies with white sectors (%r_w) are shown below the autoradiograph. Sample sizes for these genotypically wild-type strains in lanes *1*–*7* are 3240, 985, 812, 793, 831, 690, and 1095, respectively. The data for the *rap1-17* and *rif1* lanes are derived from multiple strains (including the strains displayed) representing cumulative sample sizes of >5000 and 868, respectively. Size markers (in kb) are displayed at *right*.

cells. Wild-type cells inheriting an *ADE2*-marked VII_L telomere 800–900 bp in length exhibited an elevated level of both white colonies with red sectors and red colonies with white sectors (Fig. 3, lower right; Fig. 6, 412-2c, 412-3c, 412-4d, and 412-5a). The vast majority of colonies are sectored in these strains. A similar effect is found in *rif1* mutant cells inheriting elongated telomeres from *rap1-17* cells, with the frequency of repression exceeding that found in *rif1* cells (data not shown). The hyper-repressed state is dependent on the presence of elongated telomeres. Wild-type spore colonies inheriting telomeres of approximately wild-type length (300–350 bp) from the same cross have sectoring frequencies close to wild-type (Fig. 6, 412-1c). Similarly, wild-type spore colonies containing tracts approximately wild-type in length derived from the reciprocal cross, between a wild-type strain containing the *ADE2*-marked telomere and an unmarked *rap1-17* strain, also exhibited sectoring frequencies close to wild-type (Fig. 6, 394-2d). The hyper-repressed phenotype is never observed among progeny from crosses between marked and unmarked wild-type strains (data not shown).

An analogous effect was observed at the *URA3*-marked V_R telomere (Table 2, top). Increased telomere tract length at the V_R telomere enhances the frequency of FOA^r colonies, indicating an increase in repression of the subtelomeric *URA3* gene. Telomeric tracts of >1.3

Table 2. *Telomere position effects in wild-type cells inheriting elongated V_R telomeres*

Wild-type strain	Progenitor diploid genotype	Tract size (bp)	FOA^r colonies/ 10^4 cells[a] (range of values; number of colonies)
383-3c s1[b]	*RAP1/ rap1-17*	420	0.7 (0–6.18; 10)[c]
392-2d	*RAP1/ rap1-17*	520	14.0 (1.5–119; 14)
392-6a	*RAP1/ rap1-17*	620	1.7 (0–27.9; 14)[c]
384-3a	*RAP1/ rap1-17*	650	9.7 (0.78–112; 10)
392-1c	*RAP1/ rap1-17*	670	42.0 (1.4–820; 14)
383-3c s0[b]	*RAP1/ rap1-17*	1320	320.0 (0.55–2448; 10)
384-1c	*RAP1/ rap1-17*	1420	118.0 (111–288; 4)
384-4a	*RAP1/ rap1-17*	1420	520.0 (18.9–2199; 10)
KL4-2d, −3b, −5b[d]	*RAP1/ RAP1*	300	110.0 (3–650; 30)
383-3c s0-1[e]		420	0.55
383-3c s0-3[e]		420	0.63
383-3c s0-4[e]		1180	307
383-3c s0-5[e]		1130	2448

[a]FOA^r frequencies (per 10^4 cells), presented as described in Table 1, were obtained from a population of cells having the indicated average telomere tract length.
[b]383-3c s1 is isogenic to 383-3c s0, and was derived from 383-3c s0 as a single colony after one round of subculturing (~25 generations).
[c]For 392-6a, one colony also displayed a complete absence of FOA^r cells (0/23,000 cells). For 383-3c s1, 2 of the 10 colonies displayed a complete absence of FOA^r cells (0/63,000 cells in both cases).
[d]The data derived from these strains were also presented in Table 1, line 1.
[e](s0-1, s0-3, s0-4, s0-5) Four of the 10 colonies (having the indicated FOA^r frequencies) used for the derivation of the median FOA^r frequency of 383-3c s0.

kb in size have FOA^r frequencies at or above those found in wild-type, with median values ranging between 1.2% and 5.2%. Indeed, 33% (14/44) of individual colonies have values at or above the maximum value (6.5%) observed in the original wild-type cells. In contrast, decreasing tract size to between 400 and 700 bp decreases FOA^r frequencies, with median values ranging from 0.02% to 0.4% in different segregants. In contrast to the V_R telomeres, *URA3*-marked VII_L telomeres do not display this variation in frequency, with wild-type values ranging between 25% and 50% in all spore colonies, suggesting that chromosomal context may influence the susceptibility of termini to changes in telomere size.

A further indication of a relationship between telomere size and telomere position effects is based on observations of rapid deletion events acting on the elongated telomeres inherited by wild-type cells. We have found previously that single-step deletion events can, at high frequency, eliminate substantial amounts of the elongated telomeric poly($G_{1-3}T$) tracts in *rap1-17* cells during mitotic growth (Kyrion et al. 1992). We have recently observed that wild-type cells inheriting elongated telomeres from *rap1-17* cells are also sometimes capable of producing telomeres near wild-type length in a similar single-step process (e.g., Fig. 6, 412-3c). Interestingly, the loss of 1 kb of telomeric tract at the *URA3*-marked V_R telomere is associated with a concomitant 500-fold decrease in the frequency of FOA^r colony formation, even though these cells are otherwise isogenic (Table 2, cf. 383-3c s0 and 383-3c s1). The presence of truncated telomeres helps to explain the broad distribution of FOA^r frequencies observed in 383-3c s0, because colonies that displayed reduced FOA^r frequencies (Table 2, s0-1 and s0-3) also exhibited shortened telomeres (Table 2). A similar effect was observed at *ADE2*-marked VII_L telomeres. Following rapid deletion at the VII_L telomere (e.g., Fig. 6, 412-3c), wild type cells inheriting only the deleted species lost the hyper-repressed phenotype and exhibited wild-type sectoring frequencies (data not shown). These data indicate that changes in telomere size significantly influence telomere position effects in yeast.

Discussion

Previously, we have demonstrated that *rap1^t* alleles produce truncated RAP1 molecules that, while capable of binding specifically to DNA, are missing the carboxy-terminal 144–165 amino acids (Kyrion et al. 1992). In vivo, these truncated forms of RAP1 result in telomere elongation and instability, slow growth rate, and high rates of chromosome loss and nondisjunction, suggesting that the carboxyl terminus of RAP1 plays a critical role in regulating telomere and chromosome stability. In this paper, we demonstrate that the carboxy-terminal domain of RAP1 also plays a critical role in regulating telomere-specific position effects on transcription and chromatin structure in yeast. This conclusion is based on two lines of evidence. First, truncation of the carboxy-terminal 165 or 144 amino acids of RAP1 in the *rap1-17* and *rap1-18* alleles results in the inability of telomeres to confer a transcriptionally repressed state onto adjacent polymerase II-transcribed genes. This phenotype is not the simple consequence of increased telomere tract length, because cells wild-type for *RAP1* that inherit elongated telomeres regain high levels of repression.

The second observation that argues for a critical role of the carboxyl terminus of RAP1 in telomeric suppression is the increased accessibility of subtelomeric chromatin to *dam* methylase in *rap1-17* alleles. The level of site 2 methylation at telomeric *URA3* genes is reduced significantly relative to wild-type. In this regard, the phenotype of this *rap1* mutant is similar to strains containing the *sir2* and *sir4* mutations, which display a complete loss of telomere-specific protection (Fig. 5; Gottschling 1992). However, unlike *sir2* mutants, elements of wild-type chromatin are still maintained in at least a fraction of *rap1-17* cells at both V_R and VII_L telomeres. Both strands appear to be protected against methylation in both wild-type and *rap1-17* cells (data not shown). One explanation for these results is that the fraction of DNA molecules that are methylated directly reflects the proportion of cells retaining protection against methylation. If this were true, protection against methylation could not be a sufficient criterion for forming the repressed state, because $<1 \times 10^{-7}$ cells are phenotypically Ura$^-$. Alternatively, all cells in the population may be equally affected by the *rap1-17* mutation, but the repressed state is transient and unstable, possibly as a consequence of rapid switching between chromatin conformations.

The majority of the cells assayed in wild-type, *rap1-17*, and *sir2* cells are in the derepressed state at the V_R telomere. Curiously, the nature of the derepressed state appears to be qualitatively different in *sir2* cells than in either wild-type or *rap1-17* cells, both of which have levels of protection against *dam* methylase greater than expected on the basis of their FOA^r frequencies. While confirming that the structure conferring protection against methylation is insufficient for the formation of a stable repressed state, these data raise the possibility that both wild-type and *rap1-17* derepressed cells retain elements of the closed chromatin state. In contrast, the effects of the *sir2* mutations appear to be more global in nature, eliminating all vestiges of the wild-type state.

Our data indicate that *HMLα*, but not *HMR***a**, is partially derepressed in *rap1-17* cells. These results provide the first direct evidence that RAP1 has a function in *HML* silencing, a possibility inferred previously from the functional importance of RAP1-binding sites within the *HML* silencer (Mahoney et al. 1991). We note that different cells in a population vary widely in mating efficiency. This phenotype is somewhat similar to the behavior of *sir1* mutants (Pillus and Rine 1989). The SIR1 gene product has been shown to be important for the establishment, but not maintenance, of the repressed state at *HMLα*. Whether RAP1 plays a similar role remains to be determined.

It is noteworthy that *rap1-17* mutations affect *HMLα* despite the functional redundancy present within the *HML* silencer elements. Deletion of either the E or I

silencer element has no effect on silencing (Mahoney and Broach 1989). Furthermore, deletion of the RAP1-binding site in the E box reduces mating efficiency only in the absence of the I silencer (Mahoney et al. 1991). One possible explanation for this paradox is that the weak RAP1-binding site found previously in the I element (Hofmann et al. 1989) may act as a redundant element in *HML* silencing, so that occupation of the RAP1-binding sites of both E and I elements by the terminally truncated RAP1 protein results in a loss of silencing. Alternatively, aberrant associations of RAP1 with other factors involved in the function of both E and I silencer elements (e.g., the consensus ARS element-binding complex ORC) may attenuate transcriptional repression. A third possibility is that interaction of the E and I silencers with telomeric RAP1-binding sites normally plays a role in stabilizing *HML* repression in wild-type cells. Disruption of this association in the *rap1-17* allele might then result in partial loss of E and I redundancy. In this regard, it is interesting that the I element is sufficient for repression when located at its genomic locus, but not when present on a circular plasmid, possibly reflecting an interaction between the I element and the telomere (Feldman et al. 1984; Mahoney and Broach 1989). Whether the participation of RAP1 in *HML* silencing is related to its role in telomere position effects remains unknown.

The phenotypes of the *rap1*^{t} alleles on telomere position effects are most consistent with a direct involvement of RAP1 mediated through binding to the telomere. However, some indirect models for the effect of the *rap1-17* mutation need to be considered. First, the *rap1-17* allele may indirectly influence the expression of another gene important for this process (or, alternatively, hyperactivate the telomerically located gene). However, the fact that transcription of the *MAT*α gene, which is regulated by RAP1 (Giesman et al. 1991; Kurtz and Shore 1991), is only slightly influenced by the *rap1-17* allele makes this possibility unlikely. Second, the slow growth rate of *rap1*^{t} cells could contribute to the phenotypes observed here. Although we cannot fully exclude this possibility, we note that wild-type cells grown on minimal and complete media, which vary twofold in growth rate, do not differ in position effects. In addition, we have recently identified missense alleles of *rap1* that completely derepress telomeric gene expression while not affecting growth rate (C. Liu and A. Lustig, unpubl.). Finally, it is conceivable that a lowered abundance of the Rap1-17 protein influences position effects. This possibility is unlikely, however, as the levels of DNA-binding (per microgram of extract) are identical in wild-type and *rap1-17* extracts over a broad range of substrate concentrations (G. Kyrion and A. Lustig, unpubl.).

The requirement of the carboxy-terminal region of RAP1 in telomere position effects is likely to reflect critical associations with other position–effect-related factors. Consistent with this proposal is that overproduction of the carboxyl terminus of RAP1 also results in a loss of position effects at the telomere, arguing that a limiting factor important for this process is titrated by the plasmid (E. Wiley and V. Zakian, pers. comm.). One candidate for such a factor is the RAP1-interacting protein RIF1, which plays a role in *HMR***a** silencing (Hardy et al. 1992b). However, our studies indicate that loss of RIF1 function actually increases the efficiency of repression. This effect is likely to be a general phenomenon, as an independent study analyzing the effect of *rif1* null alleles on telomere position effects at a *URA3*-marked VII_L telomere produced similar results (E. Wiley and V. Zakian, pers. comm.). Two models may explain these data. First, RIF1 may normally act to antagonize the formation or stabilization of the repressed state, possibly by competing with a second factor (e.g., one of the *SIR* gene products) for association with the carboxyl terminus. Such a competition between factors may help to explain the metastable nature of telomere position effects. Second, the longer telomeres present in *rif1* cells (Hardy et al. 1992b; see Fig. 6) may enhance position effects analogous to the behavior of wild-type cells inheriting elongated telomeres from *rap1-17* cells.

The results presented here provide the first evidence that telomere position effects are sensitive to the structure of the telomere itself. Two overlapping processes appear to influence telomere position effects in wild-type cells. First, position effects at both VII_L and V_R telomeres in wild-type cells are exquisitely sensitive to the size of the inherited marked telomere. Longer telomeres increase the frequency of repression. This size dependency is in striking contrast to the decreasing efficiency of position effects with increasing distance from the telomere (Renauld et al., this issue). These data suggest that the efficiency of telomere position effects may be governed by both the distance of the gene from the telomere tract and the length of that tract. Conceivably, telomere size may promote position effects by creating additional binding sites for either RAP1 or other telomere-binding proteins necessary for this process. An alternative, but not mutually exclusive, possibility is that longer telomeres are more capable of forming higher order structures (e.g., DNA loops) that may be important for telomere position effects.

The size dependency of position effects reopens the issue as to whether position effects may be exerted by poly($G_{1-3}T$) tracts at internal positions. A previous study (Gottschling et al. 1990) demonstrated that 80 bp of poly($G_{1-3}T$), while able to repress telomeric genes, did not influence gene expression at an internal site. Given the profound effect of telomere size on position effects, the possibility that longer tracts may repress transcription even at internal sites needs to be reexamined.

Telomere position effects also appear to be influenced by other structural changes occurring in *rap1-17* cells, unrelated to telomere size. Wild-type cells inheriting *rap1-17* V_R telomeres of near-wild-type size display a reduced efficiency of *URA3* repression relative to the original wild-type strains. The impact of these changes appears to be telomere specific, with the *URA3* gene at V_R being far more sensitive to these effects than either the *ADE2* or *URA3* gene at VII_L. Although the basis of this effect remains unknown, both its reversibility by in-

creased tract size and its genetic linkage to the V_R telomere (data not shown) suggest that a permanent change in telomere structure or sequence, rather than a mutation in a second gene, is responsible for this reduced efficiency. Such effects occurring in *rap1-17* cells may help to explain the observation that in some cases, the efficiency of telomere position effects varies even for tracts of similar size (e.g., Table 2, cf. 392-6a with 392-2d). Given the effects of both telomere size and structure on telomere position effects, it is likely that the protein–DNA interactions present at the telomere are actively involved in establishing or maintaining the transcriptionally repressed state and, consequently, in governing the chromatin structure of subtelomeric domains.

Permanent changes in telomere structure or sequence, such as those noted above, may contribute to the derepressed state observed in *rap1-17* cells. However, it seems unlikely that such effects fully account for the *rap1-17* phenotypes, as a fully derepressed state is observed in *rap1-17* cells immediately upon inheriting either a V_R or VII_L wild-type telomere and does not change regardless of the degree of subculturing or telomere size. We suggest, therefore, that RAP1 participates directly in conferring telomere position effects, possibly through facilitating the formation of telomeric chromatin structures essential for this process.

Materials and methods

Plasmids

Plasmids pVII-L–URA3–TEL, pV-R–URA3–TEL, padh4::URA3, and pADADE2(+), used for the construction of telomeric and internal copies of *URA3* and *ADE2*, have been described previously (Gottschling et al. 1990). pDP6–dam is a *LYS2*-containing integrating plasmid carrying the *E. coli dam* methylase gene (Gottschling 1992). pKL1 was derived from pDP6–dam by insertion of the *HIS3* gene into the *Bgl*II site of the *LYS2* gene. pJEF1332, a *TRP1*-containing integrating plasmid carrying the *ura3Δ1* deletion allele, has been described previously (Boeke et al. 1987).

Plasmid pRS313/RAP1 was derived by cloning an *Eco*RI–*Xba*I fragment carrying the *RAP1* gene into the *HIS3*-containing centromeric plasmid pRS313 (Sikorski and Hieter 1989). pRS313/rap1-17 was derived in a similar fashion using the *Eco*RI–*Xba*I fragment of $pRS316_H$/rap1-17 (Kyrion et al. 1992). Plasmid pRS306/his4/ADE2 was constructed by cloning a *Sal*I–*Bam*HI fragment of *HIS4* into the polylinker of the *URA3*-containing integrating plasmid pRS306 (Sikorski and Hieter 1989). The 3.6-kb *Bam*HI fragment containing the *ADE2* gene was then cloned into the polylinker of pRS306/his4, creating the plasmid pRS306/his4/ADE2.

Yeast strains and growth

Methods for yeast growth and manipulations were performed as described (Sherman et al. 1986). The yeast strains used for this study are shown in Table 3. Unless otherwise indicated, all strains are isogenic to the wild-type strain W303. The structure of the strains described below was confirmed by Southern and (where appropriate) genetic analyses. To construct strains containing the *URA3*-marked V_R telomere, and the *URA3*- and *ADE2*-marked VII_L telomeres, the wild-type strain AJL275-2a, isogenic to W303, was transformed with linearized pV-R–URA3–TEL, pVII-L–URA3–TEL, and pADADE2 (+) as described (Gottschling et al. 1990), giving rise to strains AJL275-2a–V_R, AJL275-2a–VII_L-URA, and AJL275-2a–VII_L-ADE, respectively. Isogenic strains containing an *adh4::URA3* disruption on VII_L (AJL275-2a–adh::URA) were constructed as described (Gottschling et al. 1990).

The *rap1-17* and *rap1-18* mutations were introduced into strains containing a *URA3*- or *ADE2*-marked telomere or a *URA3*-marked *adh4* locus by appropriate crosses with AJL275-2a–V_R, AJL275-2a–VII_L-URA, AJL275-2a–VII_L-ADE, and AJL275-2a–adh::URA. AJL369-4d/RAP1 was constructed by transforming the *rap1-17*-containing spore colony AJL369-4d with pRS313/RAP1.

To generate strains carrying the *ura3Δ1* allele, KL5-5a was transformed with *Stu*I-digested pJEF1332. A transformant, carrying tandem copies of the *ura3Δ1* gene (generated by gene conversion during integration), was backcrossed to generate a wild-type spore colony (AJL398-5a) containing the *ura3Δ1* allele. This strain was used to generate wild-type and *rap1-17* strains carrying both the *URA3*-marked VII_L telomere and the *ura3Δ1* allele.

A *sir2::TRP1* null allele was introduced into strains KL4-5b and AJL387-5a as described (Shore et al. 1984). The *rif1::URA3* allele was introduced into W303a as described (Hardy et al. 1992b), and subsequently crossed into wild-type and *rap1-17* strains containing the *ADE2*-marked VII_L telomere. Strains containing both the *rif1::URA3* allele and the *ADE2* gene inserted at the *HIS4* locus were identified after sporulation of a diploid derived from a cross between a *rif1::URA3*-containing strain and strain GK30. GK30, containing an integrated copy of *ADE2* at the *HIS4* locus, was generated by transformation of *Nhe*I-digested pRS306/his4/ADE2 into W303α.

To generate *rap1-17 HML***a** *MAT***a** *HMR***a** strains, a *rap1-17*-containing strain was crossed to the nonisogenic *HML***a** *MAT***a** *HMR***a** *HO* strain K828. Tetrads from this diploid segregated 2 : 2 for slow growth rate, indicating that *rap1-17* is penetrant in these backgrounds. Slow-growing colonies that were capable of mating only with an α-mating tester strain were identified. Southern analysis of DNA isolated from these candidates was used to identify strains carrying either the *HML*α or *HML***a** allele.

To introduce the *E. coli dam* methylase gene, pKL1 was linearized by digestion with *Stu*I, which cleaves uniquely within the *LYS2* gene, and the DNA was transformed into the *rad1*-containing strain W839-6b. His^+ transformants having the *dam* methylase gene integrated into the *LYS2* locus (W839-6b–dam) were identified and crossed to appropriate strains to generate wild-type and *rap1-17* strains containing a *URA3*-marked V_R or VII_L telomere and the methylase gene. The introduction of the *dam* methylase and *rad1* mutations into these strains had no effect on the expression of the telomeric *URA3* genes.

To generate wild-type strains having *ADE2*-marked VII_L telomeres 800–900 bp in length, a *rap1-17* strain containing a VII_L telomere of ~1000 bp was crossed to W303a, and the resulting diploid (AJL412) was sporulated. To generate wild-type strains having *URA3*-marked V_R telomeres 500–1500 bp in length, a *rap1-17* strain containing a V_R telomere of ~750 bp was crossed to W303a, and the resulting diploid (KL3) was sporulated. The *rap1-17* spore colony KL3-1b was subcultured on solid media for four rounds (s0–s4), with each round consisting of ~25 generations of growth (Kyrion et al. 1992). The average telomere tract lengths of KL3-1b s0, KL3-1b s1, KL3-1b s2, and KL3-1b s4 were 0.85, 1.1, 1.35, 1.45, and 1.85 kb, respectively. Each strain was crossed to W303a, the resulting diploids (AJL392, AJL383,

Table 3. *Yeast strains*

Strain	Genotype
W303a[a]	*MAT***a** *RAP1 leu2-3,112 trp1 ade2-1 ura3-1 HIS3*
W303α[a]	*MATα RAP1 leu2-3,112 trp1 ade2-1 ura3-1 his3*
AJL275-2a–VR	*MATα RAP1 leu2-3,112 trp1 ade2-1 ura3-1 his3* VR::*URA3*
AJL275-2a–VIIL–URA	*MATα RAP1 leu2-3,112 trp1 ade2-1 ura3-1 his3* VIIL::*URA3*
AJL275-2a–VIIL–ADE	*MATα RAP1 leu2-3,112 trp1 ade2-1 ura3-1 his3* VIIL::*URA3/ADE2*
AJL275-2a–adh::URA	*MATα RAP1 leu2-3,112 trp1 ade2-1 ura3-1 his3 adh::URA3*
AJL369-4d	*MAT***a** *rap1-17 leu2-3,112 trp1 ade2-1 ura3-1 his3* VIIL::*URA3*
AJL369-4d/RAP1	*MAT***a** *rap1-17 RAP1/CEN/HIS3 leu2-3,112 trp1 ade2-1 ura3-1 his3* VIIL::*URA3*
AJL369-5b	*MAT***a** *rap1-17 leu2-3,112 trp1 ade2-1 ura3-1 HIS3* VIIL::*URA3*
AJL399-4b	*MATα rap1-18 leu2-3,112 trp1 ade2-1 ura3-1 his3* VIIL::*URA3*
AJL364-1c	*MATα rap1-17 leu2-3,112 trp1 ade2-1 ura3-1 his3 adh::URA3*
W839-6b–dam	*MAT***a** *RAP1 leu2-3,112 trp1 ade2-1 ura3-1 his3 rad1::LEU2 LYS2:dam/HIS3:lys2*
KL4-5b	*MATα RAP1 leu2-3,112 trp1 ade2-1 ura3-1 his3 rad1::LEU2 LYS2:dam/HIS3:lys2* VR::*URA3*
KL5-2c	*MATα rap1-17 leu2-3,112 trp1 ade2-1 ura3-1 his3 rad1::LEU2 LYS2:dam/HIS3:lys2* VR::*URA3*
KL5-5a	*MAT***a** *rap1-17 leu2-3,112 trp1 ade2-1 ura3-1 his3 rad1::LEU2 LYS2:dam/HIS3:lys2* VR::*URA3*
KL4-5b Δsir2	*MATα RAP1 sir2::TRP1 leu2-3,112 trp1 ade2-1 ura3-1 his3 rad1::LEU2 LYS2:dam/HIS3:lys2* VR::*URA3*
AJL387-5a	*MAT***a** *RAP1 leu2-3,112 trp1 ade2-1 ura3-1 his3 rad1::LEU2 LYS2:dam/HIS3:lys2* VIIL::*URA3*
AJL391-1c	*MATα rap1-17 leu2-3,112 trp1 ade2-1 ura3-1 his3 rad1::LEU2 LYS2:dam/HIS3:lys2* VIIL::*URA3*
AJL387-5a Δsir2	*MAT***a** *RAP1 sir2::TRP1 leu2-3,112 trp1 ade2-1 ura3-1 his3 rad1::LEU2 LYS2:dam/HIS3:lys2* VIIL::*URA3*
GK23-1b[b]	*MATα RAP1/CEN/TRP1 rap1::LEU2 leu2-3,112 trp1 ade2-1 ura3-1 his3* VR::*URA3*
P17 s4[b]	*MATα rap1-17/CEN/HIS3 rap1::LEU2 leu2-3,112 trp1 ade2-1 ura3-1 his3* VR::*URA3*
P17 s4D-P[b]	*MATα RAP1/CEN/TRP1 rap1::LEU2 leu2-3,112 trp1 ade2-1 ura3-1 his3* VR::*URA3*
AJL398-5a	*MATα RAP1 leu2-3,112 trp1 ade2-1 ura3Δ1:TRP1:ura3Δ1 his3 rad1::LEU2 LYS2:dam/HIS3:lys2*
AJL401	*MATα RAP1 leu2-3,112 trp1 ade2-1 ura3Δ1:TRP1:ura3Δ1 his3 RAD1 LYS2:dam/HIS3:lys2* VIIL::*URA3* *MAT***a** *RAP1 leu2-3,112 trp1 ade2-1 ura3-1 his3 rad1:LEU2 LYS2* *MATα RAP1 leu2-3,112 trp1 ade2-1 ura3Δ1:TRP1:ura3Δ1 HIS3 RAD1 LYS2:dam/HIS3:lys2* VIIL::*URA3*
AJL406	*MAT***a** *rap1-17 leu2-3,112 trp1 ade2-1 ura3-1 his3 rad1:LEU2 LYS2*
EMPY75[c]	*MATα thr3 met*
EMPY76[c]	*MAT***a** *lys1*
AJL274-4c, AJL278-4d[d]	*MAT***a** *rap1-17 leu2-3,112 trp1 ade2-1 ura3-1 HIS3*
AJL274-3c[d]	*MATα RAP1 leu2-3,112 trp1 ade2-1 ura3-1 HIS3*
AJL274-1c, AJL278-1a[d]	*MATα rap1-17 leu2-3,112 trp1 ade2-1 ura3-1 HIS3*
K828[e]	*HML***a** *MAT***a** *HMR***a** *HO leu2 ura3 cry1*
AJL395, AJL396	*MATα RAP1 RIF1 leu2-3,112 trp1 ade2-1 ura3-1 HIS3* VIIL::*URA3/ADE2* *MAT***a** *RAP1 rif1::URA3 leu2-3,112 trp1 ade2-1 ura3-1 his3*
AJL394/AJL412[f]	*MATα RAP1 leu2-3,112 trp1 ade2-1 ura3-1 HIS3* VIIL::*URA3/ADE2* *MAT***a** *rap1-17 leu2-3,112 trp1 ade2-1 ura3-1 his3*
KL3-1b	*MATα rap1-17 leu2-3,112 trp1 ade2-1 ura3-1 his3* VR::*URA3*
AJL392	KL3-1b s0 × W303a
AJL383	KL3-1b s1 × W303a
AJL384	KL3-1b s2 × W303a
AJL386	KL3-1b s4 × W303a

[a]Strain from Kurtz and Shore (1991).
[b]The wild-type strains GK23-1b and P17 s4D-P, although genotypically identical, differ by 750 bp in tract length at the V_R-marked telomere.
[c]Gift of Dr. Eric Phizicky (University of Rochester, New York).
[d]From Kyrion et al. (1992).
[e]Gift of Dr. Amar Klar (NCI, Frederick, MD); this strain also has mutations in the *HIS2* and/or *HIS4* genes.
[f]AJL394 and AJL412 differ only in the tract length of the *ADE2*-marked VII_L telomere. AJL394 was derived by crossing a wild-type strain carrying an *ADE2*-marked VII_L telomere to an unmarked *rap1-17* strain; AJL412 was derived by crossing a *rap1-17* strain carrying elongated *ADE2*-marked VII_L telomeres to an unmarked wild-type strain (see Materials and methods).

AJL384, and AJL386, respectively) were sporulated, and wild-type spore colonies, containing V_R telomeres of differing sizes, were identified.

Telomere tract length determination

The telomere tract length of *URA3*-marked V_R and VII_L telomeres were determined as described (Kyrion et al. 1992). The tract lengths of *ADE2*-marked VII_L telomeres were determined by probing Southern blots of *Nde*I-digested DNA with a 3.6-kb *Bam*HI fragment carrying the *ADE2* gene. *Nde*I cleaves ~750 bp from the *ADE2*/poly($G_{1-3}T$) junction.

Plasmid shuffles

Following transformation of GK23-1b with pRS313/rap1-17, strains were identified that retained only the pRS313/rap1-17

plasmid. One such strain (P17) was subcultured and cells containing a V_R telomere tract length of 1.5 kb (P17s4) were transformed with pD130, containing a wild-type copy of *RAP1* on a *TRP1* centromeric plasmid (Kurtz and Shore 1991). Following nonselective growth, strains were identified that contain only the wild-type copy of *RAP1* (P17s4D-P) while retaining the elongated telomeres from *rap1-17*. We note that the lower level of repression observed when a wild-type *RAP1* gene is located in a plasmid, rather than chromosomal, context is the probable consequence of altered expression of the plasmid-encoded product.

Assays for transcriptional repression

FOA assay To assay wild-type Ura$^-$ frequencies, 4 to 10 colonies were grown on YPD media at 25°C to a diameter of 1 mm, and the entire colony was suspended and diluted in SC media. Following appropriate dilutions, cells were spread onto FOA plates and incubated at 30°C for 3–5 days. To assay Ura$^-$ frequencies in *rap1-17* , *rap1-18* and *sir2::TRP1* cells, 10 colonies were grown to a diameter of 2 mm and the entire colony (containing 1×10^7 to 4×10^7 cells), following suspension, was plated onto two FOA plates. Plates were incubated at 30°C for 5–7 days. In each case, total cell counts were determined after plating appropriate dilutions onto YPD media. The data are presented as median values together with the range of values observed. The repressed state present in both wild-type and *rap1-18* cells is reversible. FOA^r cells switch to the Ura$^+$ phenotype at high frequencies during growth on nonselective media.

ADE2 visual assay Wild-type, *rap1-17*, *rif1::URA3*, and *rap1-17 rif1::URA3* strains carrying the VII_L telomere (or *his4* locus) marked by the *ADE2* gene were grown at 30°C for 2 days. Cells were suspended in SC media, diluted, and plated onto SC media containing limiting concentrations of adenine (Hieter et al. 1985). Wild-type and *rif1::URA3* strains were grown at 30°C for 3 days and then shifted to 25°C for full color development. *rap1-17* and *rap1-17 rif1::URA3* strains were grown at 30°C for 5 days before being shifted to 25°C.

Transcriptional analysis RNA was isolated by standard methods after growth in YPD at 25°C. Following electrophoresis of RNA on a 1.5% formaldehyde–agarose gel, Northern analysis was carried out using either a *Pst*I–*Sma*I fragment derived from the *URA3* gene or a 4.0-kb *Hin*dIII fragment carrying the *MAT*α gene as a probe.

dam *methylation analysis*

DNA was isolated from *dam* methylase-containing wild-type, *rap1-17*, and *sir2* cells grown in rich (YPD) media at 25°C, and digested as described in the text, and the resulting blots were probed with the *Pst*I–*Sma*I fragment of *URA3*. This fragment has identical homology to both the telomeric and internal copies of *URA3* (see Fig. 5). The relative hybridization signals of the fragments were estimated using the β-scope (Betagen). Under some conditions of growth, yeast strains carrying the *dam* methylase exhibited a generalized decrease in methylation, leading to an overall increase in the abundance of *Dpn*I-resistant fragments. We therefore used both the *Dpn*I digestion pattern of yeast DNA and the ability of the internal fragment A to be fully cleaved by *Dpn*I as internal controls for cellular *dam* methylase activity.

Quantitative mating assays

Quantitative mating assays were carried out as described previously (Dutcher and Hartwell 1982), using *MAT***a** and *MAT*α derivatives of wild-type and *rap1-17*-containing strains, and the tester strains EMPY 75 and EMPY 76. The wild-type strain W303a was included in each trial as a control. As an additional control, six *HML***a** *MAT***a** *HMR***a** and four *HML*α *MAT***a** *HMR***a** spore colonies derived from the same diploid strain were also tested. Whereas *HML*α strains showed significant decreases in mating, *HML***a** derivatives always exhibited wild-type mating efficiencies.

Acknowledgments

We thank Dan Gottschling, David Shore, Jef Boeke, Phil Hieter, Amar Klar, and Rodney Rothstein for providing plasmids and yeast strains, and Emily Wiley, Virginia Zakian, Dan Gottschling, and David Shore for communicating results prior to publication. We also thank Titia deLange, Dale Dorsett, and E. B. Hoffman for valuable comments on the manuscript, and Ken Boakye for expert technical assistance. These studies were supported by a grant from the National Science Foundation (DMB 9120208) and our Cancer Center support grant (NCI-P30-CA-08748).

The publication costs of this article were defrayed in part by payment of page charges. This article must therefore be hereby marked "advertisement" in accordance with 18 USC section 1734 solely to indicate this fact.

References

Aparicio, O., B. Billington, and D. Gottschling. 1991. Modifiers of position effect are shared between telomeric and silent mating-type loci in *S. cerevisiae*. *Cell* **66:** 1279–1287.

Bell, S. and B. Stillman. 1992. ATP-dependent recognition of eukaryotic origins of DNA replication by a multiprotein complex. *Nature* **357:** 128–134.

Boeke, J., J. Trueheart, G. Natsoulis, and G. Fink. 1987. 5-fluoroorotic acid as a selective agent in yeast molecular genetics. *Methods Enzymol.* **154:** 164–175.

Brand, A., G. Micklem, and K. Nasmyth. 1987. A yeast silencer contains sequences that can promote autonomous plasmid replication and transcriptional activation *Cell* **51:** 709–719.

Buchman, A., W. Kimmerly, J. Rine, and R. Kornberg. 1988. Two DNA-binding factors recognize specific sequences at silencers, upstream activating sequences, autonomously replicating sequences, and telomeres in *Saccharomyces cerevisiae*. *Mol. Cell. Biol.* **8:** 210–225.

Conrad, M., J. Wright, A. Wolf, and V. Zakian. 1990. RAP1 protein interacts with yeast telomeres in vivo: Overproduction alters telomere structure and decreases chromosome stability. *Cell* **63:** 739–750.

Dutcher, S. and L. Hartwell. 1982. The role of *Saccharomyces cerevisiae CDC* genes in nuclear fusion. *Genetics* **100:** 175–184.

Feldman, J., J. Hicks, and J. Broach. 1984. Identification of the sites required for repression of a silent mating type locus in yeast. *J. Mol. Biol.* **178:** 815–834.

Giesman, D., L. Best, and K. Tatchell. 1991. Role of RAP1 in the regulation of the MATα locus. *Mol. Cell. Biol.* **11:** 1069–1079.

Gottschling, D. 1992. Telomere-proximal DNA in *Saccharomyces cerevisiae* is refractory to methyltransferase activity in vivo. *Proc. Natl. Acad. Sci.* **89:** 4062–4065.

Gottschling, D., O. Aparicio, B. Billington, and V. Zakian. 1990. Position effect at *S. cerevisiae* telomeres: Reversible repression of PolII transcription. *Cell* **63:** 751–762.

Hardy, C., D. Balderes, and D. Shore. 1992a. Dissection of a carboxy-terminal region of the yeast regulatory proein RAP1

with effects on both transcriptional activation and silencing. *Mol. Cell. Biol.* **12:** 1209–1217.

Hardy, C., L. Sussel, and D. Shore. 1992b. A RAP1-interacting protein involved in transcriptional silencing and telomere length regulation. *Genes & Dev.* **6:** 801–814.

Hieter, P., C. Mann, M. Snyder, and R. Davis. 1985. Mitotic stability of yeast chromosomes: A colony color assay that measures nondisjunction and chromosome loss. *Cell* **40:** 381–392.

Hofmann, J., T. Laroche, A. Brand, and S. Gasser. 1989. RAP-1 factor is necessary for DNA loop formation in vitro at the silent mating type locus *HML*. *Cell* **57:** 725–737.

Klein, F. T. Laroche, M. Cardenas, J. Hoffmann, D. Schweizer, and S. Gasser. 1992. Localization of RAP1 and topoisomerase II in nuclei and meiotic chromosomes of yeast. *J. Cell. Biol.* **117:** 935–948.

Kurtz, S. and D. Shore. 1991. RAP1 protein activates and silences transcription of mating-type genes in yeast. *Genes & Dev.* **5:** 616–628.

Kyrion, G., K. Boakye, and A. Lustig. 1992. C-terminal truncation of RAP1 results in the deregulation of telomere size, stability, and function in *Saccharomyces cerevisiae*. *Mol. Cell. Biol.* **12:** 5159–5173.

Laurenson, P. and J. Rine. 1992. Silencers, silencing and heritable transcriptional states. *Microbiol. Rev.* **56:** 543–560.

Levis, R., T. Hazelrigg, and G. Rubin. 1985. Effects of genomic position on the expression of transduced copies of the white gene in *Drosophila*. *Science* **229:** 558–561.

Longtine, M., N. Wilson, M. Petracek, and J. Berman. 1989. A yeast telomere binding activity binds to two related telomere sequence motifs and is indistinguishable from RAP1. *Curr. Genet.* **16:** 225–239.

Lustig, A., S. Kurtz, and D. Shore. 1990. Involvement of the silencer and UAS binding protein RAP1 in regulation of telomere length. *Science* **250:** 549–553.

Mahoney, D. and J. Broach. 1989. The HML mating-type cassette of *Saccharomyces cerevisiae* is regulated by two separate but functionally equivalent silencers. *Mol. Cell. Biol.* **9:** 4621–4630.

Mahoney, D., R. Marquardt, G.-J. Shei, A. Rose, and J. Broach. 1991. Mutations in the *HML E* silencer of *Saccharomyces cerevisiae* yield metastable inheritance of transcriptional repression. *Genes & Dev.* **5:** 605–616.

Pillus, L. and J. Rine. 1989. Epigenetic inheritance of transcriptional states in *S. cerevisiae*. *Cell* **59:** 637–647.

Sherman, F., G. Fink, and J. Hicks. 1986. *Methods in yeast genetics*. Cold Spring Harbor Laboratory, Cold Spring Harbor, New York.

Shore, D., M. Squire, and K. Nasmyth. 1984. Characterization of two genes required for the position-effect control of yeast mating-type genes. *EMBO J.* **3:** 2817–2823.

Shore, D., D. Stillman, A. Brand, and K. Nasmyth. 1987. Identification of silencer binding proteins from yeast: Possible roles in *SIR* control and DNA replication. *EMBO J.* **6:** 461–467.

Sikorski, R. and P. Hieter. 1989. A system of shuttle vectors and yeast host strains designed for efficient manipulation of DNA in *Saccharomyces cerevisiae*. *Genetics* **122:** 19–27.

Singh, J. and A. Klar. 1992. Active genes in budding yeast display enhanced in vivo accessibility to foreign DNA methylases: A novel in vivo probe for chromatin structure of yeast. *Genes & Dev.* **6:** 186–196.

Sussel, L. and D. Shore. 1991. Separation of transcriptional activation and silencing functions of the *RAP1*-encoded repressor/activator protein 1: Isolation of viable mutants affecting both silencing and telomere length. *Proc. Natl. Acad. Sci.* **88:** 7749–7753.

Wright, J., D. Gottschling, and V. Zakian. 1992. *Saccharomyces* telomeres assume a nonnucleosomal chromatin structure. *Genes & Dev.* **6:** 197–210.

RAP1 and telomere structure regulate telomere position effects in Saccharomyces cerevisiae.

G Kyrion, K Liu, C Liu, et al.

Genes Dev. 1993, **7:**
Access the most recent version at doi:10.1101/gad.7.7a.1146